ELSEVIER

Theoretical and Applied Fracture Mechanics 35 (2001) 69–79

theoretical and applied fracture mechanics

www.elsevier.com/locate/tafmec

Fatigue and fretting fatigue of ion-nitrided 34CrNiMo6 steel

J.D. Costa *, J.M. Ferreira, A.L. Ramalho

ICEMS, Faculty of Science and Technology, Department of Mechanical Engineering, University of Coimbra (DEM/FCTUC), Pinhal de Marrocos, 3030 Coimbra, Portugal

Abstract

This work is concerned with the surface treatment (ion nitriding) of fretting fatigue and fatigue resistance of 34CrNiMo6. Tests are made on a servo-hydraulic machine under tension for both treated and non-treated specimens. The test parameters involve the applied displacements $\delta \pm 80$–± 170 μm; fretting pressure $\sigma_n = 1000$–1400 MPa; fatigue stress amplitude $\sigma_a = 380$–680 MPa and stress ratio $R = -1$. The ion nitriding process improves both fatigue and fretting fatigue lives. Subsurface crack initiation from internal discontinuities was found for ion-nitrided specimens.

Keywords: Fretting fatigue; Surface treatments

1. Introduction

Plasma (or ion) nitriding is preferred when compared with gas nitriding. The advantages involve the ability to select either an ε or a γ monophase layer or even elimination of the white layer, lower treatment temperatures, and improved control of case thickness [1]. The heat treatment makes it easier to control the dimensions and in some cases eliminate machining all together [1].

Fatigue strength can be significantly improved by nitriding. The formation of precipitates in the diffusion layer tends to increase the hardness and create compressive residual stresses. These beneficial stresses lowers the magnitude of the applied tensile stresses and hence increase the fatigue life of the component.

Response of material to nitriding depends on the alloying elements. Low alloy steels belong to the class of materials which have strong nitriding-forming elements such as chromium and molybdenum. The initial microstructure can also influence the nitriding process. For alloy steels, a quenched and tempered structure gives the best result [1].

Fretting fatigue involves initiation and propagation. Crack nucleation could occur without external loading and significantly reduce the initiation life. The fretting parameters that impede early cracking are the normal load contact stress and the imposed displacement amplitude. Once an embryo crack is nucleated and starts to grow in stage II, fracture mechanics could be applied to estimate the rate of crack growth. Fretting fatigue cracks ordinarily grow in Mode I. However, majority of the component life under fretting fatigue is consumed during the initiation stage [2]. Hence,

* Corresponding author. Tel.: +351-239-790700; fax: 351-239-790701.

E-mail addresses: jose.domingos@mail.dem.uc.pt (J.D. Costa), martins.ferreira@mail.dem.uc.pt (J.M. Ferreira), amilcar.ramalho@mail.dem.uc.pt (A.L. Ramalho).

0167-8442/01/$ - see front matter
PII: S0167-8442(00)00050-1

fretting fatigue is an initiation-controlled process. What needs to be better understood is the nature of initiation and its influence on fretting.

Fatigue life reduction of different materials due to fretting has been studied [3–6]. Normal pressure due to contacting surfaces often decreases the fatigue life with the excepcion of the work in [5].

Three fretting fatigue regimes have been identified. They include stick, gross slip and mixed stick-slip. In the range of macroslip, the frictional force is relatively independent of slip and the asperities are sliding over each other. As the slip amplitude increases, the fretting fatigue strength either increases [7] or reaches a constant value [8].

Several researchers studied the effect of ion nitriding on fatigue behaviour [9,10]. In general, improvements of fatigue resistance were found for the stress-controlled high-cycle regime. Beneficial effect of ion nitriding on fatigue was attributed to hardness increase of the surface and increase surface residual stress. Additional investigations are needed.

2. Experimental details

Fatigue and fretting fatigue tests were conducted on the 34CrNiMo6 steel. Its chemical composition is given in Table 1. The mechanical properties (after quenching and tempering) are given in Table 2. One series of specimens were submitted to surface treatment by ion nitriding. The treatment conditions are indicated in Table 3. The depths of the treated layers were about 0.35 mm according to the DIN 50190 part 3 standard. The white layer had a depth of about 5–7 μm and X-ray diffraction analysis revealed that both $\varepsilon(Fe_2–3N)$ and $\gamma(Fe_4N)$ phases were present in this layer.

All tests were carried out in tension in a servo-hydraulic machine with load control. Specimen details are shown in Fig. 1(a). According to the ASTM E466-82 standard [11], the specimens were machined from a bar with 16 mm diameter. The geometry of the fretting pads obtained from the same material is also shown in Fig. 1(b).

Both untreated and treated specimens were submitted to fatigue tests to study the effect of the surface modification treatment on the fatigue resistance. The results will be presented by the S–N curves. These tests were taken under load control condition at a frequency of 10 Hz using a sinusoidal waveform and a stress ratio R of -1. The load was monitored using a load cell. The number of cycles up to fracture was taken. Fretting fatigue tests were also conducted for treated and untreated

Table 1
Chemical composition of 34CrNiMo6 steel (%)

C	Cr	Mn	Si	Mo	Ni	Fe
0.34	1.55	0.55	0.27	0.22	1.55	Balance

Table 2
Mechanical properties of 34CrNiMo6 steel

Yield strength (Mpa)	Tensile strength (MPa)	Elongation to rupture (%)	Hardness HV
1100	1250	10	365

Table 3
Nitrogen ion implantation treatment

Temperature (°C)	Time (h)	White layer		Diffusion layer
		Hardness ($HV_{0.2}$)	Thickness (μm)	Thickness (mm)
530	6	900	10	0.35

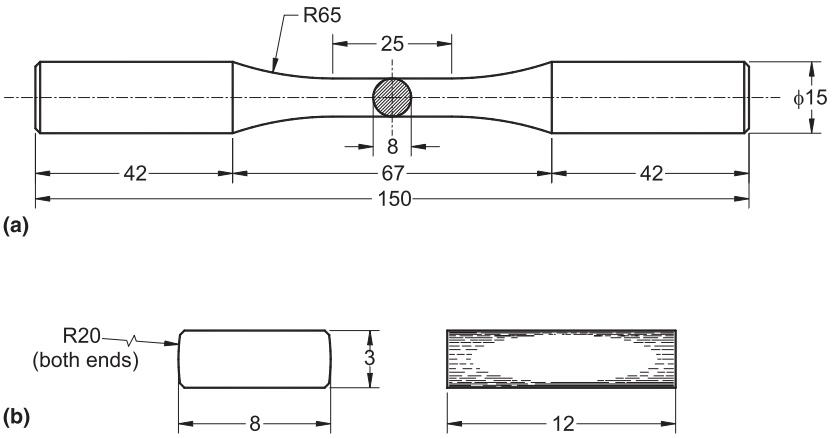

Fig. 1. (a) Fatigue and fretting fatigue specimens; (b) fretting pad. Dimensions in mm.

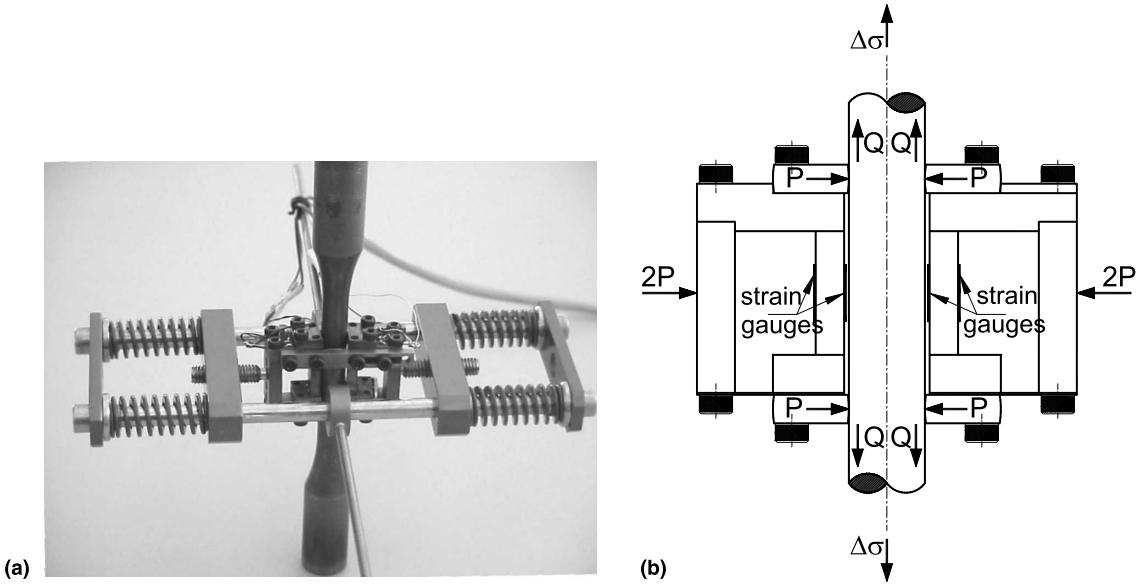

Fig. 2. Fretting fatigue apparatus: (a) photo; (b) schematic.

specimens. Fig. 2(a) shows a photo of the apparatus and Fig. 2(b) gives the corresponding schematic for the center portion.

The tangential force was dynamically monitored using four extensometers bonded on the apparatus in a complete Wheatstone bridge. The tangential displacement on the pads makes contact with the axial elongation of the specimen; the relatively high stiffness of the pads rig restrain the relative movement between the top and bottom pads. The imposed oscillatory motion between the pads and the specimens are connected to the oscillatory fatigue stress of the specimen. For a stress range of $\Delta\sigma = 1000$ MPa, and a distance between contacts of $L_0 = 24$ mm, the measured relative displacement is $\delta_m = 114$ μm. During the test, the normal force P, the tangential force Q and the axial force F_a were recorded. Refer to Fig. 3(a).

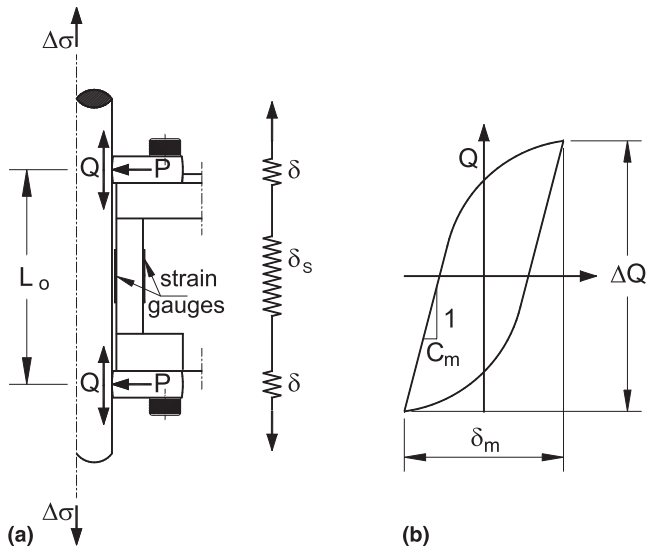

Fig. 3. Schematic representation of the compliance of the system: (a) fatifue loading; (b) Q vs δ record..

The magnitude of the tangential force as a function of theoretical relative displacement (estimated from the axial fatigue load) was recorded for each cycle. The compliance of the system C_S was determined by subtracting the theoretical contact compliance of the two contact points from the measured compliance. Inverse of the tangent to the linear part of the circuit record $Q-\delta$ is illustrated in Fig. 3(b)

$$C_S = C_m - 2 \times \frac{1}{8c} \times 2\left(\frac{2-v}{G}\right), \tag{1}$$

where c is the semimajor axis of the elliptical contact area, v the Poisson coefficient and G is the transverse elasticity modulus.

The calculated elongation of the specimen between the pad contacts is (PL_0/AE). The measured displacement is δ_m and the displacement on the apparatus is δ_S. Hence, the contact displacement δ on each pad can be estimated as

$$\delta = \left(\frac{\delta_m - \delta_S}{2}\right) = \left(\frac{\delta_m - C_S Q}{2}\right). \tag{2}$$

The contact geometry is shown in Fig. 1. The pressure distribution is given by Hertz theory of contact [12]. The relationship between the maximum compressive stress S_c on the contact and the applied load P_n is

$$S_c = 310.4 P_n^{1/3}. \tag{3}$$

Specimens and pads were machined and polished to a surface finish $R_a = 0.12$–0.17 μm. After nitriding, the specimens shows a greater value of the roughness $R_a = 0.55$–0.65 μm. The controlling parameters are the imposed displacements δ_m from ≈80 to ≈180 μm; fretting normal stress σ_n within the range 1000–1400 MPa; and fatigue stress range $\Delta\sigma = 380$–690 MPa. Table 4 summarises the parameters used in the various fretting fatigue of tests.

Table 4
Parameters used on the series of fatigue and fretting fatigue tests

Test	Normal stress (MPa)	Slide amplitude (μm)	Fatigue stress amplitude (MPa)
Fatigue			480–690
Fretting fatigue	1000 1200 1400	±80–±180	380–500

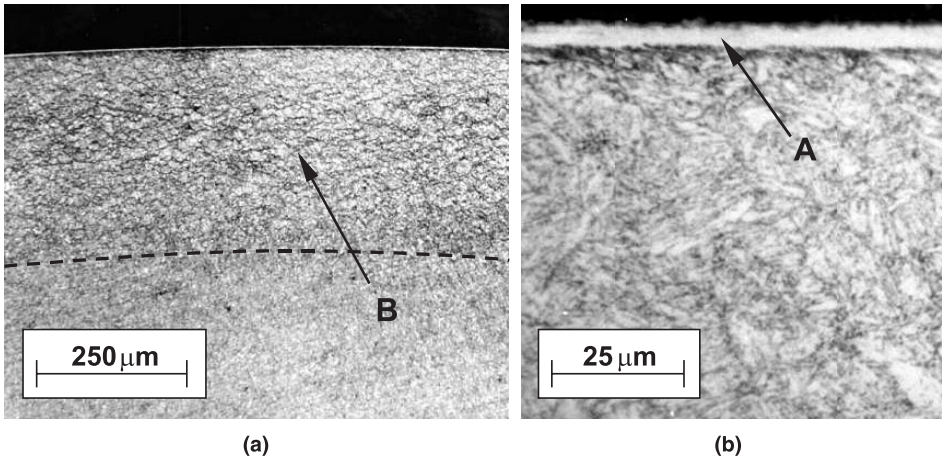

Fig. 4. Microstructure of the nitrided layers 34CrNiMo6 steel: (a) view of total treated layer; (b) detailed view of the white layer and microstructure of the diffusion layer.

In order to identify the degradation mechanisms, the fatigue surfaces were examined by scanning electron microscopy. The tests were made at room temperature (20°C) and relative humidity between 40% and 50%.

3. Results and discussion

Figs. 4(a) and (b) show two photos of the cross-section of the treated specimens. The two typical layers created by the nitrogen ion implantation can be clearly seen. The white surface layer is very thin; it has a thickness of about 10 μm. Below this, a second thicker layer is seen; it is the diffusion layer. The hardening process is obtained by nitrogen interstitial solution and formation of some phases by combination with other alloy elements in the steel. The thickness of the nitrided layer is about 0.35 mm.

Fatigue life is normally improved by increasing the surface hardness with a surface treatment. Vickers microhardness was evaluated at the cross-section of the specimens for both treated and non-treated specimens. The results are plotted in Fig. 5 against the distance from the surface. A maximum value of hardness of about 900 HV was observed near the surface within the white layer. In the diffusion layer, the hardness decreases with the distance from the surface. For depths above 0.6 mm, the hardness remains at 365 HV. The microhardness measurements were repeated for several specimens and no significant differences were found.

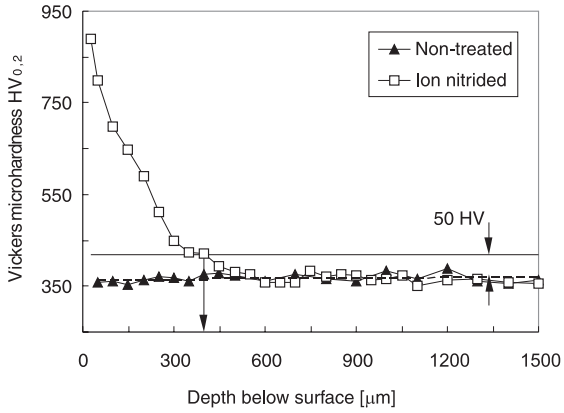

Fig. 5. Microhardness profiles for both ion-nitrided and non-treated specimens.

Comparing the hardness of the treated and the untreated specimens for depths greater than 0.60 mm, similar values of about 365 HV were observed. There was no decrease of hardness in the treated specimens. This is possibly caused by tempering that could have occurred during nitrogen ion implantation. It is important to note this because a lost of hardness in the core of the treated

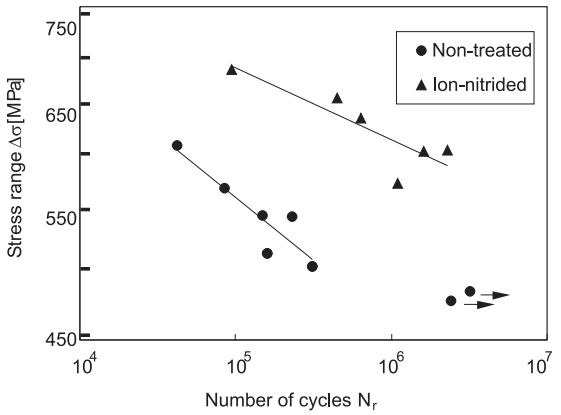

Fig. 6. Experimental fatigue results and average S–N curves.

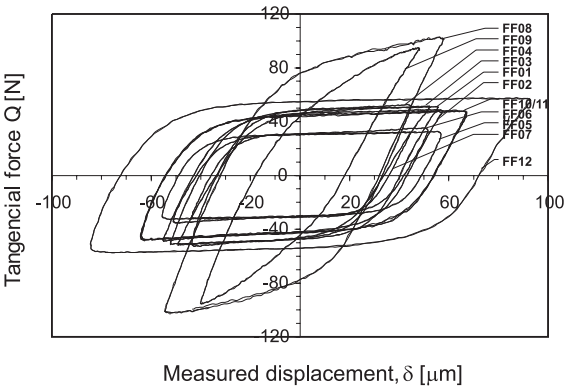

Fig. 7. Hysteresis loops of the tangential force Q versus measured displacement δ_m.

specimens could suppress the initiation of a subsurface crack.

Four series of tests were carried out. Each series consists of more than six tests covering the range 10^4 and 10^7 cycles. The results are plotted in Fig. 6 for untreated and treated specimens. Plotted are the stress range against the number of cycles to failure. The treated specimens show a higher fatigue resistance than the untreated specimens.

For the same material subjected to bending at $R = 0$, previous work [13] showed only a slight improvement of fatigue resistance. For lives below 10^5 cycles, a decrease of fatigue resistance was observed. This was attributed to the formation of a very hard white layer that is brittle. Crack initiation was enhanced by cleavage, specially for high applied maximum stress with $R = 0$.

Fig. 7 shows some stabilised loops of the tangential force Q versus measured displacement δ for different values of normal pressure P_n and slide amplitude δ. Table 5 gives values of the relevant parameters for the specimens referred in Fig. 7. One of these parameters is the energy ratio E_d/E_t, where E_d is the energy dissipated during a loading cycle and E_t is the total fretting cycle energy ($2Q\delta$), which is one of the criteria used to determine the

Table 5
Test conditions and results of the fretting fatigue tests on the non-treated condition

Ref. specimen	$\Delta\sigma$ (MPa)	σ_n (MPa)	δ_m (μm)	δ (μm)	No. of cycles	Tangent force, Q (N)	Friction coeff., μ	E_d (N μm)	E_t ($2\delta_m Q$) (N μm)	E_d/E_t
FF01	964.5	1200	110	43	92 553	51	0.88	7544	11 310	0.667
FF02	992.3	1200	113	44	65 505	48.5	0.84	7448	11 113	0.670
FF03	905.7	1200	103	37	85 543	51.5	0.89	6294	10 736	0.586
FF04	771.6	1200	88	34	252 910	52	0.90	6278	9313	0.674
FF05	984.3	1000	112	48	86 819	32	0.95	5777	7353	0.786
FF06	898.4	1000	103	42	108 794	34.5	1.03	5109	7300	0.700
FF07	774.7	1000	88	37	209 808	32	0.95	4288	5771	0.743
FF08	982.3	1400	112	34	40 850	101	1.10	11 002	23 127	0.476
FF09	771.6	1400	88	19	85 063	95	1.04	4953	16 819	0.295
FF10	771.6	1200	132	54	90 558	47	0.81	9175	12 850	0.714
FF11	765.5	1200	131	54	172 897	47	0.81	9143	12 561	0.728
FF12	776.3	1200	177	73	758 000	56.5	0.97	15 300	20 448	0.748
						Average	0.93			
					Standard deviation		0.09			

regime of fretting [14]. It can be concluded that all the tests were made in the gross slip regime characterised by an energy ratio greater than 0.2. Only the FF09 test has an energy ratio of 0.295; it is close to the mixed stick-slip regime. One condition for the existence of the fretting regime is that the ratio between the contact amplitude and the length of contact in the direction of sliding must be less than unity. For the tests in this work, the ratio is between 0.07 and 0.3.

Fig. 8 shows the evolution of the friction coefficient with the number of cycles. The significant variation occurred within the first 100 cycles where a large increase of the friction coefficient is observed. Thereafter, a fluctuation is observed. These variations always occur during the first thousands of cycles. The maximum values of the friction coefficient attained in each test are given in Table 5. A reduced scatter can be obtained for a mean value of 0.93 with a standard deviation of 0.09.

Results of fretting fatigue of untreated specimens are plotted in the Fig. 9. It shows plots of the stress range against the number of cycles to failure for three normal loads σ_N. The S–N curves are also shown for comparison. Note that fretting fatigue interaction decreases the resistance of the material for the untreated condition. As the normal load increases from 1200 to 1400 MPa, the fretting fatigue life decreases. This is expected. For $\sigma_N = 1000$ and 1200 MPa, the fretting fatigue lives

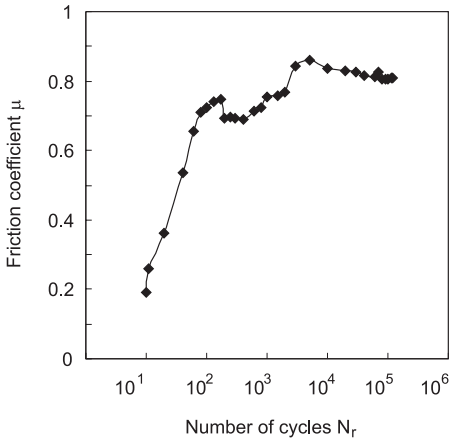

Fig. 8. Variation of the friction coefficient with the number of cycles ($\sigma_n = 1200$ MPa; $\delta_m = 131$ μm).

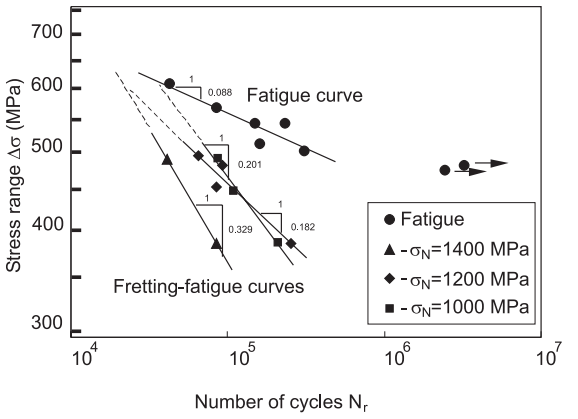

Fig. 9. Experimental fretting fatigue results for the non-treated condition.

does not change significantly. This behaviour is not in agreement with the work in [5,15], which reports the existence of a normal pressure threshold for fretting fatigue, above which the pressure does not affect the fatigue life. The corresponding values of pressure in the present tests are the maximum Hertzian compressive stresses. They reduce significantly as the area of the contact surface increase by wear. For typical values of surface area observed at the end of the fretting fatigue tests, the pressures were 22, 38 and 61 MPa, respectively, for Hertzian maximum stresses of 1000, 1200 and 1400 MPa. Between 1000 and 1200 MPa, the variation between the final pressures is about 16 MPa. Between 1200 and 1400 MPa, the variation is about 23 MPa. This explains, in part, the influence of the normal pressure. The influence however is not consistent and more tests are needed for an explanation.

The values of the exponent on the Basquin relation were observed to be very different for the two types of tests: −0.088 for the fatigue tests and −0.18 to −0.33 for the fretting fatigue tests. Values as high as these obtained in fretting fatigue tests are very close to the inverse of the Paris coefficient m for steels ($m = 4$–6). Therefore, crack propagation life is more important in the fretting fatigue tests than that in the plain fatigue tests. The initiation phase occupies only a small part of the specimen life.

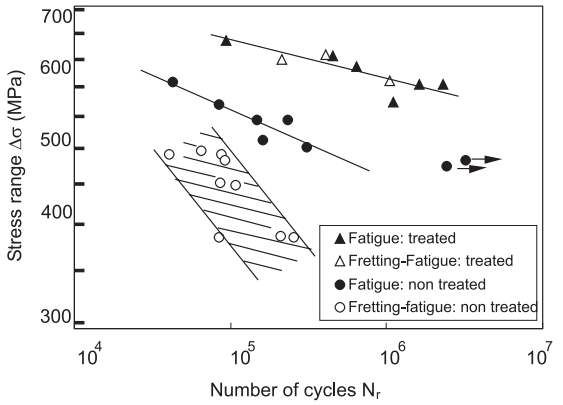

Fig. 10. Experimental fretting fatigue and fatigue results for both conditions.

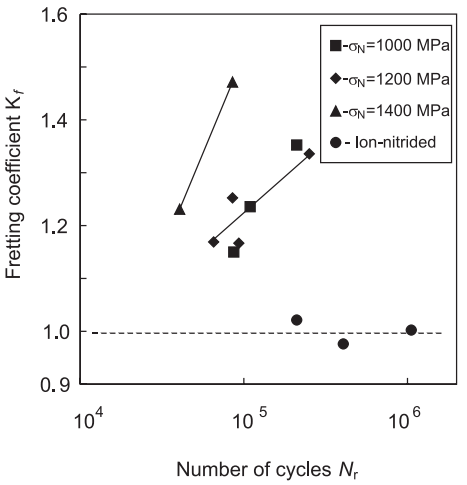

Fig. 11. K_f as a function of the number of cycles to failure for the non-treated and ion-nitrided specimens.

Fig. 10 summarises all the fretting fatigue and fatigue results for both treated and untreated specimens. No difference was observed between the fretting fatigue lives and the corresponding fatigue lives for the treated specimens. For those specimens subjected to the ion nitriding process, crack initiation always occurs from an internal inclusion. This applies to the fatigue tests and fretting fatigue tests. The treatment increases the fretting fatigue strength of the specimen surface to a level such that crack initiation from internal inclusions is enhanced as compared with initiation from the fretting scars. Fig. 11 presents the dependence of the fretting coefficient K_f on the number of cycles to failure. It is defined as the ratio between the maximum stresses σ_R and $\sigma_{R,f}$ for each cycle for smooth specimens and specimens subjected to fretting fatigue. Fretting reduces the fatigue resistance of the untreated specimens by a factor between 1.15 and 1.5. The fretting coefficient K_f increases with the number of cycles to fracture. For the specimens treated with ion-nitride, the fretting influence is almost insignificant with K_f close to unity.

For the untreated specimens, cracks tends to initiate at the edge of the fretting zone, where the stress concentration is higher. Fig. 12 shows the

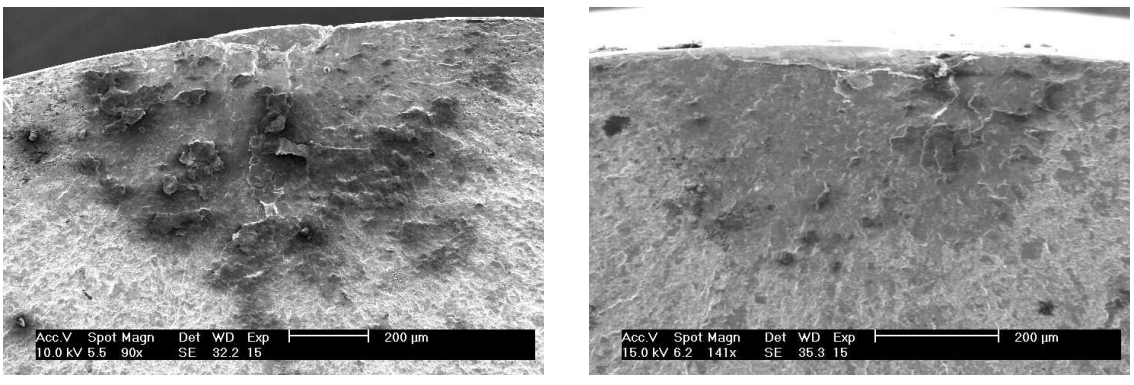

(a) (b)

Fig. 12. SEM photomicrographs of the crack initiation in the non-treated specimens: (a) first example; (b) second example.

results of two examples. Debris of oxidation can be observed on the fatigue surfaces. Formed are the fretting scars that are probably transported to the fatigue surfaces by the slide movement between the pad and the specimen. For the specimens with ion nitride, crack is always initiated below the surface, starting from an inclusion, not only for the fatigue tests but also for the fretting fatigue tests. Figs. 13(a)–(c) present three typical examples of the photomicrographs obtained by scanning electron microscopy. Fig. 13(d) gives a detailed view of crack initiation from an inclusion. For a homogeneous material, the process of fatigue initiation usually starts from a free surface following the intrusion and extrusion mechanism produced by sequential slip of two intersecting slip planes. However, in specimen treated by ion-nitride, this process is impeded by the increased hardness of the surface layer. As a consequence, cracks can initiate easier from internal discontinuities. Many investigators have shown that subsurface crack initiation is associated with non-metallic inclusions [16]. Although measurements of residual stresses were not carried out in this work, their presence is

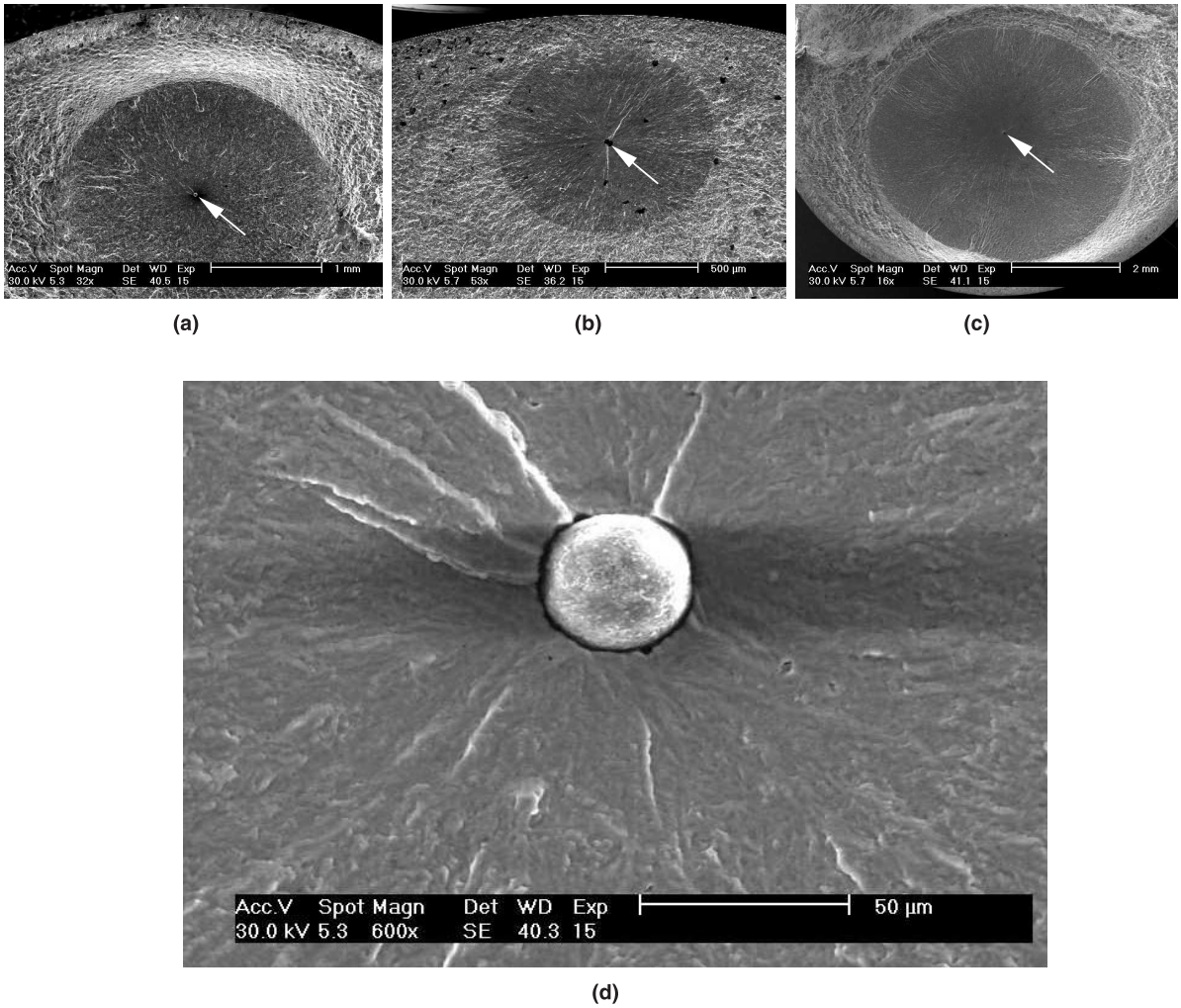

Fig. 13. SEM photomicrographs of crack initiation at inclusions in the ion-nitrided specimens. White arrows indicate origin of the crack initiation: (a) $\sigma_{max} = 602$ MPa; $N_f = 1,620,630$; (b) $\sigma_{max} = 687$ MPa; $N_f = 94,600$; (c) $\sigma_{max} = 572$ MPa; $N_f = 1,098,200$; (d) detailed view of photomicrograph (a).

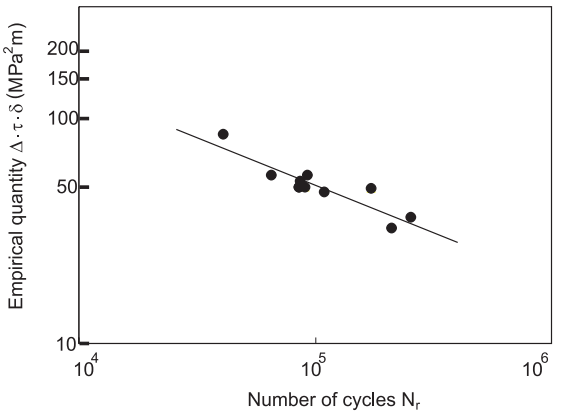

Fig. 14. Fretting fatigue parameter $\Delta\sigma\tau\delta$ against the number of cycles to failure.

expected during the ion-nitriding treatment. The formation of nitrides in a layer could cause a volume increase. This is restrained by the core causing a state of compression and tensile in the core. The action of compression tends to reduce the tensile action in fatigue.

Investigators [6,17] have used a combination of applied fatigue stress, frictional tangential stress and normal pressure as fretting fatigue parameters. They consider these as the cause of damage that lead to eventual to nucleation and propagation of fatigue cracks. Models have been proposed to suggest that tangential stress increases with the normal pressure. This would cause a decrease in the fretting fatigue life of the components. The possible existence of the pressure threshold tends to limit the application of these models. One of these models will be used. Fig. 14 shows the results, where the empirical parameter $\Delta\sigma\tau\delta$ is plotted against the number of cycles to failure. Here, $\Delta\sigma$ is the fatigue stress range, τ the tangential stress and δ is the slide displacement on the contact. Despite the scatter, a decreasing trend of the $\Delta\sigma\tau\delta$ parameter with increasing N_r is clear.

4. Conclusions

- The process of ion nitriding improves fatigue resistance of the 34CrNiMo6 steel in the range of lives analysed. The treatment increases the hardness of the surface layer and introduces compressive residual stress preventing crack initiation in the surface layer. As a consequence, crack initiation occurs from internal discontinuities for applied stresses higher than those of the untreated specimens. This explanation is supported by SEM of the fatigue surfaces.
- Fretting fatigue lives of untreated specimens were significantly lower than those specimens treated with ion nitride. Crack initiation in the fretting fatigue of specimens treated with ion-nitride also occurs from internal discontinuities. Hence, fretting damage does not seem to influence the life of the specimen.
- An influence of the normal pressure was observed between 1200 and 1400 MPa. However, for the lower values of the stress range 1000–1200 MPa, the fretting fatigue values are very close. More tests are needed before a conclusion could be made in the influence of normal stress.

Acknowledgements

The present work has been supported by the Portuguese Government Project Praxis XXI 2/2.1 TPAR 2041/95. It is very important for us that this last modification can be considered. We want to tanks in advance.

References

[1] M. James, O. Brien, D. Goodman, Plasma (Ion) Nitriding, ASM International, Metals Park, OH, 1995, pp. 420–424.
[2] D.A. Hiils, D. Nowell, J.J. O'Connor, On the mechanics of fretting fatigue, Wear 125 (1988) 129–146.
[3] C. Petiot, L. Vincent, K. Dang Van, N. Maouche, J. Foulquier, B. Journet, An analysis of fretting fatigue failure combined with numerical calculations to predict crack nucleation, Wear 181–183 (1995) 101–111.
[4] O. Vingsbo, D. Soderberg, On fretting maps, Wear 126 (1988) 131–147.
[5] S. Adibnazari, D. Hoepper, A fretting fatigue normal pressure threshold concept, Wear 160 (1993) 33–35.
[6] M.H. Wharton, R.B. Waterhouse, The effect of different contact materials on the fretting fatigue strength of an aluminium alloy, Wear 26 (1973) 253.
[7] D.J. Gaul, D.J. Duquette, The effect of fretting and environment on fatigue crack initiation and early propa-

gation in quenched and tempered 4130 steel, Metall. Trans. A 11 (1980) 1555–1561.
[8] A.J. Fenner, J.E. Field, La fatigue dans les conditions de frottement, Rev. Metall. 55 (1958) 478–485.
[9] J. Quian, A. Fatemi, Cyclic deformation and fatigue behaviour of ion-nitrided steel, Int. J. Fatigue 17 (1995) 15–24.
[10] X. Luan, Z. Li, B. Wang, in: T. Spalvins, W.L. Kovacs (Eds.), Ion nitriding and iron carburizing, ASM International, Metals Park, Ohio, 1990, pp. 257– 262.
[11] ASTM E466-82, Standard practice for conducting constant amplitude axial fatigue tests of metallic materials, Annual Book of ASTM Standards, vol. 03.01, American Society for Automotive Engineers, 1993.
[12] K.L. Jonhson, Contact Mechanisms, Cambridge University Press, Cambridge, 1985.
[13] M.G. Carreira, J.M. Ferreira, A.L. Ramalho, J.D. Costa, Fretting fatigue on the surface hardened 34CrNiMo6 steel, in: Proceedings of Euromat'98 Materials on Oceanic Environment, vol. II, Lisbon, Portugal, 22–24 July 1998, pp. 89–98.
[14] S. Fouvry, P. Kapsa, L. Vincent, Analysis of sliding behaviour for fretting loading: determination of transition criteria, Wear 185 (1996) 35–46.
[15] G.L. Goss, D.W. Hoeppner, Normal loads effects in fretting fatigue of titanium and aluminium alloys, Wear 27 (1974) 153.
[16] P. Starker, H. Wohlfart, E. Macherauch, Fat Fract. Eng. Mater. Struct. 1 (1979) 319.
[17] K. Endo, H. Goto, Initiation and propagation of fretting fatigue cracks, Wear 38 (1976) 311.